



This is the accepted manuscript made available via CHORUS. The article has been published as:

Harmonically confined math xmlns="http://www.w3.org/1998/Math/MathML">mi>n/mi>/math>-electron systems coupled to light in a cavity: Time-dependent case

Chenhang Huang, Cody Covington, and Kálmán Varga Phys. Rev. B **107**, 235130 — Published 14 June 2023

DOI: 10.1103/PhysRevB.107.235130

# Harmonically confined N-electron systems coupled to light in a cavity: time-dependent case

Chenhang Huang, 1 Cody Covington, 2 and Kálmán Varga<sup>1,\*</sup>

An analytically solvable time-dependent coupled light-matter problem is presented. An N-electron system is confined by a harmonic oscillator potential and interacts with photons in a cavity. Both the electrons and the photons can interact with a time-dependent external field. The light-matter coupling is described by the Pauli-Fierz Hamiltonian. By separating the relative and center-of-mass motion, the Hamiltonian of the system can be simplified to a sum of a Hamiltonian of the relative and the center-of-mass motion. The Hamiltonian of the relative motion is time-independent, not coupled to light, and can be solved by conventional approaches. The Hamiltonian of the center-of-mass motion reduces to that of a time-dependent harmonic oscillator and can be solved analytically. The analytical solution will be used to study excitations, high harmonic generation spectrum, and nonlinear optical properties in a cavity.

### I. INTRODUCTION

The interaction of light and matter in cavities is very successfully described by the Jaynes-Cummings (JC) model [1]. The predictions of the JC model have been experimentally tested [2–4] and new physical effects, for example, Rabi oscillations [5], Fock states [6–8], squeezed states [9], entanglement of atoms and photons [10], Schrödinger cat states [11], and anti-bunching [12, 13] are predicted.

The JC model was also extended to explicitly time-dependent Hamiltonians, e.g. a classical laser field is added to drive the system [14–20]. The coupling [21] or the frequency [22] can also be time-dependent. Time-dependent JC Hamiltonians where the driving field can couple either to the atom or to the cavity mode were also studied [23]. These approaches were used to model the dynamic stark effect [23, 24], synchronization of qubits [20], photon blockade [25], entanglement generation [24, 26], highly excited Fock states [27], coherent states [28], induced atomic resonance fluorescence [29], or control of the quantum electromagnetic field [30] in cavities or superconducting circuits.

With the advance of experimental approaches the study of systems with strong and ultra-strong light-matter coupling became the center of interest [31–42]. In the ultra strong regime the approximations of the JC model are not valid and a new level of theoretical description is needed. The most popular and practical approach is based on the Pauli-Fierz (PF) Hamiltonian. The PF Hamiltonian describes the interaction between quantum matters (electrons) and a massless quantized radiation field (photons) in the low-energy non-relativistic limit of quantum electrodynamics (QED) [43]. The PF approach has often been used in describing the modification of material properties in optical cavities [44–53]. In a previous paper, [54], we have shown that the PF Hamiltonian

is analytically solvable for a harmonically confined twoelectron system. Later we extended the analytical solution to harmonically confined N-electron systems [55].

In this work, we will investigate a harmonically confined N-electron system in time-dependent driving fields. Two driving fields will be considered, an external laser pulse interacting with the electrons and an external current interacting with the photons. As the electrons and the photons are coupled, the external field acting on the electrons excite the photons and vice versa. Coupled electrons and photons in external fields haven been studied using perturbation theory [56, 57] or with numerical approaches [58]. The effect of light-matter coupling on electron-electron interaction and correlation in laser driven cavities has been investigated [59–62].

The wave function of the harmonically confined electron systems can be factorized into a relative motion and a center-of-mass motion part. The wave function of the relative motion is time-independent and it can be solved analytically for N=2 electrons [54] or numerically for N>2 electrons [55]. The center-of-mass Hamiltonian is coupled to light and it is time-dependent. This Hamiltonian can be separated into a sum of laser-driven time-dependent one-dimensional harmonic oscillator Hamiltonians. These Hamiltonians have analytic solutions, or alternatively, they can be solved by exact diagonalization and time-propagation as will be shown in this paper.

Numerical calculations will be presented to show how the time-dependent external fields can be used to excite photons and electrons. We will show that by a suitable chosen external field the system can be excited to a desired photon number state. One photon states have been experimentally generated for quantum computer applications using entangled atoms [7, 8] using. Our calculations show that states with fixed number of photons can also be created using quantum dots with harmonic confinement. The external fields can also change the high harmonic generation (HHG) spectra and the nonlinear properties of the system. The tunability of the nonlinear properties of molecules has been studied in Ref. [63] using the QED

<sup>&</sup>lt;sup>1</sup>Department of Physics and Astronomy, Vanderbilt University, Nashville, Tennessee, 37235, USA
<sup>2</sup>Department of Chemistry, Austin Peay State University Clarksville, Tennessee, 37044, USA

<sup>\*</sup> kalman.varga@vanderbilt.edu

time-dependent density functional theory [58, 64, 65]. In this work we study these effects in an analytically solvable model system. The numerical examples highlight several interesting possibilities. In the case of HHG, the coupling to the cavity can remove inversion symmetry and even harmonics can appear in the spectrum. The coupling also introduces new polaritonic excitation peaks that appear in the HHG spectrum. The position of these peaks are independent of the frequency of the exciting laser field but depend on the confining potential and the cavity parameters. Thus, the HHG spectrum can be altered by the cavity and it is not only determined by the driving field. It will be also shown that the nonlinear susceptibility can be tuned by the coupling strength and the cavity frequency. We have found that the susceptibility strongly depends on the occupation of the excited states. The occupation of the excited states can be tuned by the cavity frequency and the light matter coupling. The occupation increases with stronger coupling, but has a maximum value as a function of the frequency. The nonlinear susceptibilities follow a similar tendency.

The outline of the paper is as follows. In section II. the formalism is introduced and the separation of the Hamiltonian into exactly solvable terms is presented. In section III. the diagonalization of the coupled light center-of mass Hamiltonian is discussed. In section IV. numerical calculations for the laser-driven Hamiltonian are considered. This is followed by a short summary. Appendices are added to make the paper self-containing.

### II. FORMALISM

We assume that the system is nonrelativistic and the coupling to the light can be described by the dipole approximation (the wavelength of light is much larger than the size of the system). The non-relativistic PF QED Hamiltonian provides a consistent quantum description at this level. The PF Hamiltonian in the Coulomb gauge [44–48]:

$$H = H_e + H_{ep}$$

$$H_e = \sum_{i=1}^{N} \left( -\frac{\hbar^2}{2m_e} \vec{\nabla}_i^2 + v_{\text{ext}} (\mathbf{r}_i, t) \right) + \frac{e^2}{4\pi\epsilon_0} \sum_{i>j}^{N} \frac{1}{|\mathbf{r}_i - \mathbf{r}_j|}$$

$$H_{ep} = \sum_{\alpha=1}^{N_p} \left\{ \frac{1}{2} \left[ \hat{p}_{\alpha}^2 + \omega_{\alpha}^2 \left( \hat{q}_{\alpha} - \frac{\boldsymbol{\lambda}_{\alpha}}{\omega_{\alpha}} \cdot \mathbf{D} \right)^2 \right] + \frac{j_{\text{ext}}^{(\alpha)}(t)}{\omega_{\alpha}} \hat{q}_{\alpha} \right\}$$

$$(2)$$

where  $\mathbf{r}_i$  are the positions,  $m_e$  is the mass and e is the charge of the electrons. In Eq. (2) the photon fields are described by quantized oscillators using raising and lowering operators  $\hat{a}_{\alpha}$  and  $\hat{a}_{\alpha}^{+}$ .  $\mathbf{D}$  is the dipole operator

$$\mathbf{D} = \sum_{i=1}^{N} \mathbf{r}_i,\tag{3}$$

where N is the number of electrons and

$$q_{\alpha} = \sqrt{\frac{\hbar}{2\omega_{\alpha}}} (\hat{a}_{\alpha}^{+} + \hat{a}_{\alpha}) \tag{4}$$

is the displacement field.  $p_{\alpha}$  is the canonical conjugate momentum to  $q_{\alpha}$ , which can be written as

$$p_{\alpha} = i\sqrt{\frac{\hbar\omega_{\alpha}}{2}}(\hat{a}_{\alpha}^{+} - \hat{a}_{\alpha}). \tag{5}$$

In addition to the static terms a time-dependent external potential,  $v_{\rm ext}({\bf r}_i,t)$  interacts with the electrons and a time-dependent external current,  $j_{\rm ext}^{(\alpha)}(t)$  interacts with the photons. The Hamiltonian in Eq. (2) describes  $N_p$  photon modes with photon frequency  $\omega_{\alpha}$  and coupling  $\lambda_{\alpha}$ . The coupling term is usually written as [66]  $\lambda_{\alpha} = \sqrt{4\pi} \, S_{\alpha}({\bf r}) {\bf e}_{\alpha}$ , where  $S_{\alpha}({\bf r})$  is the cavity mode function at position  ${\bf r}$  and  ${\bf e}_{\alpha}$  is the transversal polarization vector of the photon modes.

The external potential will be taken in the form

$$v_{\text{ext}}(\mathbf{r}_{i}, t) = \frac{1}{2} m_{e}^{2} \omega_{0}^{2} \sum_{i=1}^{N} \mathbf{r}_{i}^{2} + \mathbf{E}_{\text{ext}}(t) \mathbf{D}$$

$$= \frac{1}{2} m_{e}^{2} \frac{\omega_{0}^{2}}{N} \left[ \sum_{i < j}^{N} (\mathbf{r}_{i} - \mathbf{r}_{j})^{2} + \left( \sum_{i=1}^{N} \mathbf{r}_{i} \right)^{2} \right] + \mathbf{E}_{\text{ext}}(t) \mathbf{D},$$
(6)

which is a sum of harmonic oscillator confinements and an external electric pulse described as a classical field. In the second line we have used an identity that will be useful later in this section.

Atomic units are used,  $\hbar$ , e,  $m_e$ , and  $4\pi\epsilon_0$  are all equal to unity and may be dropped from the equations.

One can define N-1 relative coordinates (see Appendix A for more details)

$$\mathbf{x}_i = \mathbf{r}_i - \mathbf{R}, \quad (i = 1, ..., N - 1), \quad \mathbf{R} = \frac{1}{N} \sum_{j=1}^{N} \mathbf{r}_j.$$
 (7)

Many different relative coordinate system can be defined (two are presented and the relation between them are discussed in Appendix A). The above choice is a particularly simple because the single particle coordinates can be expressed as

$$\mathbf{r}_{i} = \mathbf{x}_{i} + \mathbf{R}, \quad (i = 1, ..., N-1), \quad \mathbf{r}_{N} = -\sum_{j=1}^{N-1} \mathbf{x}_{j} + \mathbf{R}.$$
(8)

The Hamiltonian for the electrons can be written as

$$H_e = H_{\mathbf{x}} + H_{\mathbf{B}},\tag{9}$$

with

$$H_{\mathbf{x}} = \frac{1}{2} \sum_{i=1}^{N-1} \pi_i^2 + \frac{1}{2} \frac{\omega_0^2}{N} \sum_{i < j}^{N} (\mathbf{r}_i - \mathbf{r}_j)^2 + \frac{1}{2} \sum_{i < j}^{N} \frac{1}{|\mathbf{r}_i - \mathbf{r}_j|},$$
(10)

and

$$H_{\mathbf{R}} = \frac{1}{2N} \mathbf{P}^2 + \frac{1}{2} N \omega_0^2 \mathbf{R}^2 + N \mathbf{E}_{\text{ext}}(t) \mathbf{R}, \qquad (11)$$

where **P** is the canonically conjugate momentum to **R** and  $\pi_i$  are canonically conjugate momenta to  $\mathbf{x}_i$ . Note, that  $H_{\mathbf{x}}$  depends on  $\mathbf{r}_i - \mathbf{r}_j$  but using Eq. (8)  $\mathbf{r}_i - \mathbf{r}_j$  can be expressed using the N-1 relative coordinates  $\mathbf{x}_k$  and there is no dependence on **R**.

Assuming that we have only one photon mode with frequency  $\omega$  and defining the coupling term as  $\lambda = \lambda(1, 1, 0)$  the electron-photon coupling term becomes

$$H_{ep} = \omega \left( \hat{a}^{\dagger} \hat{a} + \frac{1}{2} \right) - N \omega \hat{q} \lambda \mathbf{R} + \frac{1}{2} N^2 \left( \lambda \mathbf{R} \right)^2 + \frac{j_{\text{ext}}(t)}{\omega} \hat{q}.$$
(12)

The generalization to many photon modes and different forms of  $\lambda$  is simple and can be found in Ref. [55]. To simplify the notation and make the paper more readable, we will restrict to a single mode and the above-defined  $\lambda$ .

Now the total Hamiltonian can be written as

$$H = H_{\mathbf{x}} + \left[\omega \left(\hat{a}^{\dagger} \hat{a} + \frac{1}{2}\right) + \frac{j_{\text{ext}}(t)}{\omega} \hat{q}\right] - N\omega q \lambda \mathbf{R} + \left(H_{\mathbf{R}} + \frac{1}{2}N^2 \left(\lambda \mathbf{R}\right)^2\right).$$
(13)

The first term is the Hamiltonian of the relative motion and it is not coupled to the center-of-mass motion or to the photon space and it is time-independent. For N=2 electrons,  $H_{\mathbf{x}}$  can be analytically solved [54], for more than 2 electrons it can be treated numerically [55].

The terms in the square bracket represent the Hamiltonian of the photons coupled to the center-of-mass through the third term  $(N\omega q\lambda \mathbf{R})$ . The terms in the round bracket represents the Hamiltonian acting on the center-of-mass motion.

As it is shown in Appendix B the Hamiltonian can be decoupled into the following form

$$H = H_{x} + H_{v} + H_{z} + H_{c}, \tag{14}$$

where

$$H_c = \omega \left( \hat{a}^{\dagger} \hat{a} + \frac{1}{2} \right) - \omega q \sqrt{2N} \lambda u + \frac{j_{\text{ext}}(t)}{\omega} \hat{q} + H_u.$$
 (15)

Here  $H_u$ ,  $H_v$  and  $H_z$  are one dimensional time-dependent harmonic oscillator functions. These are analytically solvable [67, 68] (see Appendix C) and the timedependent eigenfunctions  $\phi_v(v,t)$  and  $\phi_z(z,t)$  are known. We note, that as it is discussed in Appendix B one simplify the model further by assuming an external field defined as  $\mathbf{E}_{ext}(t) = (E(t), E(t), 0)$ . In that case  $\phi_v$  and  $\phi_z$ are time-independent harmonic oscillator functions.

The ansatz

$$\Psi = \Phi(\mathbf{x})e^{-iE_{\mathbf{x}}t}\phi_v(v,t)\phi_z(z,t)\Phi_c(u,t), \tag{16}$$

satisfies the time-dependent Schrödinger equation

$$i\frac{\partial}{\partial t}\Psi = H\Psi. \tag{17}$$

The wave functions  $\Phi_x$ ,  $\phi_v$ , and  $\phi_z$  are already known and we only need to deal with  $H_c$  as it will be discussed in the next section.

# III. DIAGONALIZATION OF THE LIGHT-MATTER COUPLED HAMILTONIAN

The Hamiltonian  $H_c$  can be diagonalized in two different ways. In the first approach, new variables are introduced to decouple the CM and photon harmonic oscillators. In the second one, a product basis of the CM and photon harmonic oscillators  $\phi_k(u)|n\rangle$  is used, where  $\phi_k(u)$  satisfies the time-independent equation

$$H_u\phi_k(u) = \left(k + \frac{1}{2}\right)\omega_u\phi_k(u), \quad \omega_u^2 = \omega_0^2 + 2N\lambda^2$$
 (18)

(see Appendix B). The advantage of the first approach is that it is exact, while numerical diagonalization is needed in the second approach. The advantage of the second approach is that the solution is directly obtained as a product of spatial and photon spaces.

# A. Shifted Fock states

The coupling Hamiltonian can be rewritten as

$$H_c = -\frac{1}{2}\frac{\partial^2}{\partial q^2} + \frac{1}{2}\omega^2 q^2 - \frac{1}{2}\frac{\partial^2}{\partial u^2} + \frac{1}{2}\omega_u^2 u^2 + \kappa uq + \epsilon_q q + \epsilon_u u,$$
(19)

with

$$\kappa = -\omega \sqrt{2N}\lambda, \quad \epsilon_q = \frac{j_{ext}(t)}{\omega}.$$
(20)

This is a Hamiltonian of two coupled time-dependent harmonic oscillators. The Hamiltonian can be decoupled by introducing the following coordinate rotations

$$r = q\cos\theta - u\sin\theta,$$
  

$$s = q\sin\theta + u\cos\theta.$$
(21)

with  $\tan 2\theta = \frac{2\kappa}{\omega_u^2 - \omega^2}$ . The Hamiltonian is decoupled into two uncoupled time-dependent harmonic oscillators

$$H_{c} = H_{r} + H_{s},$$

$$H_{r} = -\frac{1}{2} \frac{\partial^{2}}{\partial r^{2}} + \frac{1}{2} \omega_{r}^{2} r^{2} + c_{r}(t) r,$$

$$H_{s} = -\frac{1}{2} \frac{\partial^{2}}{\partial s^{2}} + \frac{1}{2} \omega_{s}^{2} s^{2} + c_{s}(t) s,$$
(23)

where

$$\omega_r^2 = \omega^2 \cos^2 \theta + \omega_u^2 \sin^2 \theta - \kappa \sin 2\theta,$$
  

$$\omega_s^2 = \omega^2 \sin^2 \theta + \omega_u^2 \cos^2 \theta + \kappa \sin 2\theta,$$
(24)

and

$$c_r(t) = \epsilon_q \cos \theta - \epsilon_u \sin \theta,$$
  

$$c_s(t) = \epsilon_q \sin \theta + \epsilon_u \cos \theta.$$
(25)

Now the analytical solution can be written as a product of the eigen functions of  $H_r$  and  $H_s$  in Eq. (23) as outlined in Appendix C.

## B. Exact diagonalization

The Hamiltonian in Eq. (15) can also be solved by exact diagonalization using the product of center-of-mass eigenfunctions and photon Fock states as basis states

$$|n_u, n_q\rangle = \phi_{n_u}(u)|n_q\rangle. \tag{26}$$

To diagonalize  $H_c$ , one needs the matrix elements of the Hamiltonian which are readily available. The operators  $H_u$  and u act on the real space, and  $\hat{a} + \hat{a}^+$  acts on the photon space. The matrix elements of q and u are

$$\langle m|q|n\rangle = \frac{1}{\sqrt{2\omega}}D_{mn},$$
 (27)

$$\langle i|u|j\rangle = \frac{1}{\sqrt{2\omega_u}}D_{ij},$$
 (28)

where

$$D_{mn} = \begin{pmatrix} 0 & \sqrt{1} & 0 & 0 & 0 & \dots \\ \sqrt{1} & 0 & \sqrt{2} & 0 & 0 & \dots \\ 0 & \sqrt{2} & 0 & \sqrt{3} & 0 & \dots \\ 0 & 0 & \sqrt{3} & 0 & \sqrt{4} & \dots \\ 0 & 0 & 0 & \sqrt{4} & 0 & \dots \\ \vdots & \vdots & \vdots & \vdots & \vdots & \ddots \end{pmatrix}.$$
(29)

Thus, the matrix elements of  $H_c$  are

$$\langle i, m | H_c | j, n \rangle = \delta_{mn} \delta_{ij} (j + \frac{1}{2}) \omega_u + \delta_{mn} \delta_{ij} (n + \frac{1}{2}) \omega + \frac{k}{2\sqrt{\omega\omega_u}} D_{mn} D_{ij} + \frac{\epsilon_u(t)}{\sqrt{2\omega_u}} D_{ij} \delta_{nm} + \frac{\epsilon_q(t)}{\sqrt{2\omega}} D_{nm} \delta_{ij}. \tag{30}$$

After the diagonalization, we have the eigenenergies and the eigenfunctions. The eigenfunction has the following form

$$\Phi_c = \sum_{n_u, n_q} c_{n_u, n_q} \phi_{n_u}(u) |n_q\rangle, \tag{31}$$

where  $c_{n_u,n_q}$  are the components of the eigenvector.

In the large N limit we have  $\omega_u \approx \sqrt{2N\lambda}$  and the coupling strength in the last term of Eq. (30) will be

$$\sqrt{\omega}(N/8)^{1/4} \tag{32}$$

which is independent of  $\lambda$ . In this case,  $\omega_u$  is very large and the lowest u harmonic oscillator state dominates

$$\Phi_c = \sum_{n_q} c_{0,n_q} \phi_0(u) |n_q\rangle. \tag{33}$$

# IV. RESULTS

In this section, we present numerical examples using the exact diagonalization approach. The advantage of this method is that the matter and photon coordinates are factorized and one can analyze the weight of the matter and light components in the wave function easily.

First one has to construct a product basis

$$\phi_{n_u}(u)|n_q\rangle,\tag{34}$$

where the highest  $n_u$  and  $n_q$  values depend on the coupling strength, on the frequency of light, and on the confining harmonic oscillator potential. One can easily find the appropriate values by testing the convergence of the lowest energies as a function of the basis dimension.

The converged ground or excited state

$$\Phi_c(t=0) = \sum_{n_u, n_q} c_{n_u, n_q} \phi_{n_u}(u) |n_q\rangle, \tag{35}$$

will be time propagated to solve the time-dependent problem. In the time propagation, the basis is timeindependent but the linear coefficients change in time and the wave function is

$$\Phi_c(t) = \sum_{n_u, n_q} c_{n_u, n_q}(t) \phi_{n_u}(u) |n_q\rangle$$
 (36)

We will use the Crank-Nicolson [69] time-propagator to solve the time-dependent Schrödinger-equation:

$$\Phi_c(t + \Delta t) = \exp(-\frac{i}{\hbar}H\Delta t)\Phi_c(t)$$
(37)

$$\approx \frac{1 - \frac{i}{2}H\Delta t}{1 + \frac{i}{2}H\Delta t}\Phi_c(t), \tag{38}$$

where H is the Hamiltonian matrix defined in Eq. (30). The Crank-Nicolson method is unconditionally stable, and with an appropriately small time step, it converges

to the exact solution [70]. In our case the dimension of H is low so the calculation of the inverse in the Crank-Nicolson step is computationally cheap, but H is very sparse and one could use iterative inversion even for H of large dimensions. Atomic units will be used in the calculations.

We will calculate the following quantities.

1. Norm of the wave function as a function of time

$$|\Phi_c(t)|^2 = \sum_{n_u, n_q} |c_{n_u, n_q}(t)|^2.$$
 (39)

This is a good measure of the accuracy of the time propagation, the norm remains one if the time step is suitably chosen and will diverge if the time step is too large.

2. The occupation probability of a given CM harmonic oscillator wave function as a function of time

$$\Phi_{cm}(n_u, t) = \sum_{n_q} |c_{n_u, n_q}(t)|^2.$$
 (40)

This function shows how the oscillator states are excited during the external time-dependent pulse.

The occupation probability of a given photon state as a function of time

$$\Phi_{ph}(n_q, t) = \sum_{n_u} |c_{n_u, n_q}(t)|^2.$$
 (41)

This shows the excitation of the photon states.

4. The time-dependent expectation value of the Hamiltonian

$$E = \langle \Phi_c(t) | H_c | \Phi_c(t) \rangle$$

$$= \sum_{n_u, n_q} \sum_{n'_u, n'_q} c_{n_u, n_q}(t)^* c_{n'_u, n'_q}(t) \langle n_u, n_q | H_c | n'_u, n'_q \rangle.$$
(42)

Note that his quantity is not constant because the energy of the electromagnetic field is not added. This quantity shows the change of the energy of a time-propagated state compared to the initial state.

5. The time-dependent dipole moment for the centerof-mass

$$u(t) = \langle \Phi_c(t) | u | \Phi_c(t) \rangle$$

$$= \frac{1}{\sqrt{2\omega_u}} \sum_{n_u, n'_u, n_q} c_{n_u, n_q}(t)^* c_{n'_u, n_q}(t) D_{n_u n'_u},$$
(43)

where  $D_{nn'}$  is defined in Eq. (29).

6. The high harmonic spectrum is calculated using the dipole acceleration:

$$I(\omega_h) = \left| \int_0^T \frac{\partial^2 u(t)}{\partial t^2} e^{-i\omega_h t} dt \right|^2.$$
 (44)

To calculate the high harmonic spectrum, we time propagate a system in a laser pulse, calculate u(t), and then  $I(\omega)$ .

7. The nonlinear susceptibilities. Using an electric field  $E_i f(t)$  that is sufficiently weak, the induced dipole moment  $u_i(t)$  can be expressed in power series [71, 72]

$$u_i(t) = \sum_{n} p^{(n)}(t) (E_i)^n,$$
 (45)

where  $p^{(n)}(t)$  is the *n*th order component of the polarization. The polarization,  $p^{(n)}$ , can be expressed using the *n*th order susceptibility  $\chi^{(n)}$  as

$$p^{(n)}(t) = \int \chi^{(n)}(t - t_1, t - t_2, \dots t - t_n) \times f(t_1) f(t_2) \dots f(t_n) dt_1 dt_2 \dots dt_n, (46)$$

and this describes the nonlinear optical properties of the system. To calculate  $\chi^{(n)}$ , one time propagates the system subject to  $E_i f(t)$  for several values of  $E_i$  and invert Eq. (45) to get  $p^{(n)}(t)$ . Then  $\chi^{(n)}$  can be extracted from (46) [71, 72].

#### A. Excitation by an external field

In this case, the system is subject to a time-dependent external field of the form

$$\epsilon_q(t) = E_e f(t)$$
  $f(t) = g(\frac{20\pi}{\omega_e}, \frac{32\pi}{\omega_e}, t) \sin(\omega_e t)$  (47)

where  $E_e$  is the strength of the excitation,  $\omega_e$  is the excitation frequency and the envelope function is defined as a trapezoidal

$$g(a,b,t) = \begin{cases} \frac{2t}{b-a} & t < \frac{1}{2}(b-a) \\ 1 & \frac{1}{2}(b-a) \le t < \frac{1}{2}(a+b) \\ 1 - 2\frac{t-\frac{a+b}{2}}{(b-a)} & t > \frac{1}{2}(a+b) \\ 0 & t > b \end{cases}$$
(48)

As Eq. (19) shows, the coupling Hamiltonian is symmetric in  $\epsilon_q$  and  $\epsilon_u$ . The former excites the photons through the coupling to the photon displacement q, and the latter excites the electrons through coupling to the dipole moment.

Fig. 1 shows the excitation caused by the external field. We will investigate the cavity frequency and the coupling strength dependence of the wave functions using the first excited state. The ground state only shows oscillation following the oscillation of the external excitation but the order of states does not change for physically realistic parameter sets. In the case of the first excited state, there are changes in level order depending on the parameters of the cavity. By appropriate choice of parameters, one can drive the system into a desired photon number state as experimentally described in Ref. [7, 8].

In Fig. 1a the first excited state and an entangled state of the photon states  $|0\rangle$  and  $|1\rangle$  is time propagated. The

oscillation of the energy and occupation numbers follows the oscillation of the laser field. The highest occupied CM harmonic oscillator occupation state oscillates between the  $n_u=0$  and  $n_u=1$  states. The order of the higher occupied photon states changes at the beginning and the end of the laser pulse. The occupation of the  $|2\rangle$  photon states also significantly increases.

In the second case (Fig. 1b),  $\lambda$  is kept the same but  $\omega$  is decreased. As Eq. (30) shows, this decreases the coupling between the CM motion and photons but increases the strength of the external field. As a consequence, the starting first excited state is almost purely a  $\Phi_c = \phi_0(u)|1\rangle$  state and the occupations of the harmonic oscillator states barely change. The occupations of the photon states and the order of the states, however, rapidly change.

In the third case, we increase  $\lambda$ . In this case, the coupling is stronger and the starting wave function ( $\Phi_c = 0.58\phi_1(u)|0\rangle + 0.78\phi_0(u)|1\rangle + 0.13\phi_2(u)|1\rangle$ ) contains higher harmonic oscillator components. The oscillation of the energy and occupation numbers become irregular because the higher harmonic oscillator and photon states get excited. Moreover, the oscillations of the occupation numbers continue after the laser pulse in a Rabi-oscillation-like manner. These examples show that changing the coupling, cavity frequency, and harmonic confinement can generate a variety of coupled light-matter states with an external field.

# B. High harmonic generation

Fig. 2 shows the high harmonic spectrum of the system calculated using Eq. (44). The system is subject to a Gaussian envelop laser pulse

$$\epsilon_u(t) = E_e f(t)$$
  $f(t) = exp(-\frac{(t-\tau)^2}{\sigma^2})\sin(\omega_e t)$  (49)

and time propagated for 100000 time units. Note that in this case the CM motion dipole is excited by  $\epsilon_u$  (see Eq. (30)). Fig. 2a shows the HHG for the non-coupled,  $\lambda=0$ ,  $\omega=0$  case. Due to the inversion symmetry of the CM harmonic oscillator Hamiltonian, only the odd harmonics appear in the spectrum at  $n\omega_e$  for  $n=1,3,5,\ldots$  Once the light and matter degrees of freedom are coupled (Figs. 2b,2c, and 2d), the inversion symmetry is lost and even harmonics can appear depending on the coupling and the cavity frequency.

Fig. 2 shows (blue arrows) the position of the excitation energies of the lowest eigenstates of the time-dependent Hamiltonian (defined by the first three terms in Eq. (30)). If the coupling is weak then the first two terms of Eq. (30) determine the eigenenergies. The dipole operator couples states  $\phi_i|n\rangle$  and  $\phi_j|m\rangle$  if n=m and  $j=i\pm 1$ . (see Eq. (30)).

In case of no coupling, the lowest states are  $\phi_0|0\rangle$ ,  $\phi_1|0\rangle$ ,  $\phi_2|0\rangle$  and the excitation energies shown in Fig. 2a are  $\omega_u$  and  $2\omega_u$  (the excitation energy is defined by

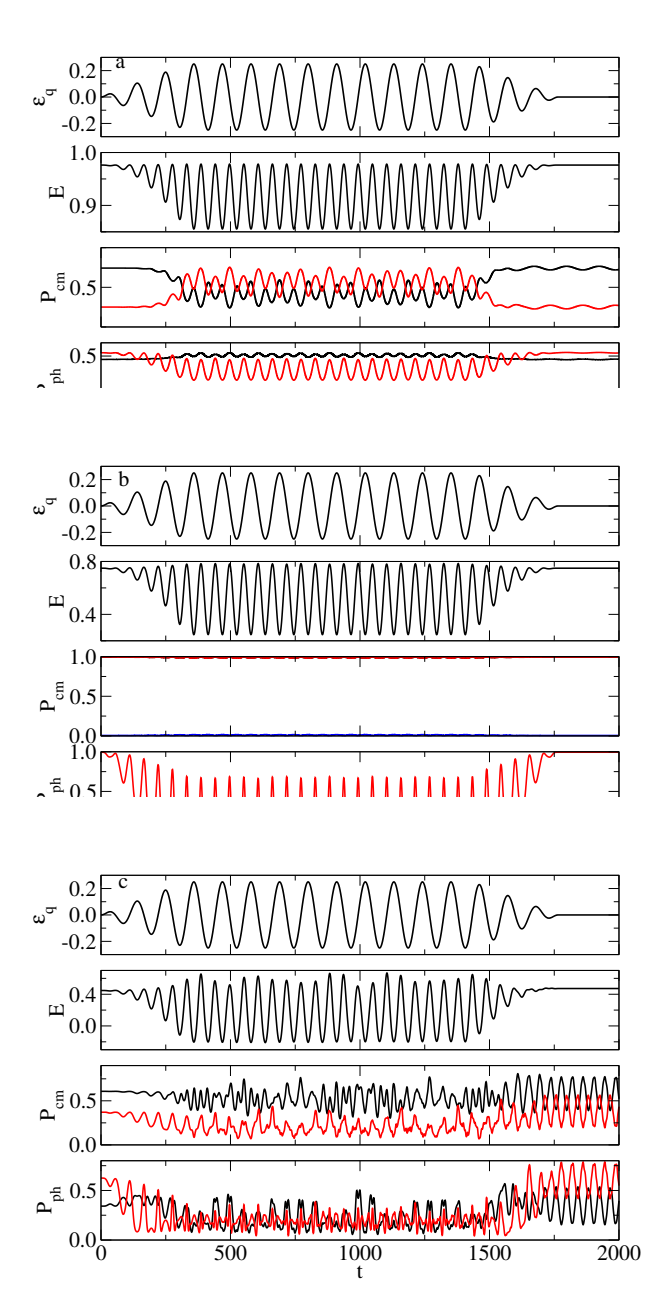


FIG. 1. Time propagation of the light-matter coupled system. (a) External pulse, energy, center-of-mass, and photon number occupation probability as a function of time for N=2 electrons with  $\omega_0 = 0.5$ ,  $\omega = 0.5$  and  $\lambda = 0.025$ . The starting state is the first excited state,  $\Phi_c = 0.69\phi_1(u)|0\rangle + 0.72\phi_0(u)|1\rangle$ . (b) External pulse, energy, center-of-mass, and photon number occupation probability as a function of time for N=2 electrons with  $\omega_0 = 0.5$ ,  $\omega = 0.25$  and  $\lambda = 0.025$ . The starting state is the first excited state,  $\Phi_c = \phi_0(u)|1\rangle$ . (c)External pulse, energy, center-of-mass, and photon number occupation probability as a function of time for N=2 electrons with  $\omega_0 = 0.25$ ,  $\omega = 0.25$  and  $\lambda = 0.075$ . The starting state is the first excited state,  $\Phi_c = 0.58\phi_1(u)|0\rangle + 0.78\phi_0(u)|1\rangle + 0.13\phi_2(u)|1\rangle$ .  $\omega_e = 0.057$  is used in the calculations. In the occupation number figures, the black curve corresponds to quantum number 0, the red to 1, the green to 2, and the blue to 3. The green and blue are not shown in c because they would overlap the other curves.

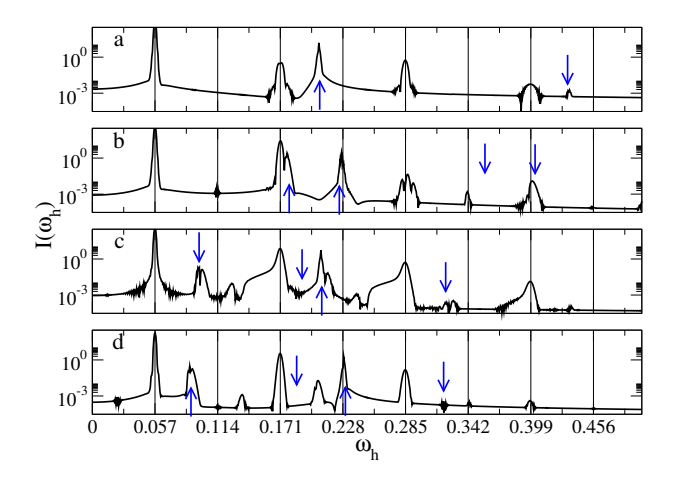


FIG. 2. High harmonic spectra. a: No coupling; b:  $\omega = 0.2$ ,  $\lambda = 0.025$ ; c:  $\omega = 0.1$ ,  $\lambda = 0.025$ ; d:  $\omega = 0.1$ ,  $\lambda = 0.05$  The exciting laser is defined by Eq. (49) with  $E_e = 0.2$ ,  $\omega_e = 0.057$ ,  $\tau = 5067$   $\sigma = 2067$ , and T = 100000. The red and blue bars show the positions of the excitation energy of the lowest states of the time-independent system. The excitation energy is defined as the difference between the energy of the excited state minus the energy of the ground state.

subtracting the ground state energy from the energy of the given state). One can see that a peak appears at the position of the excitation energies corresponding to the transitions from the ground state to the excited states due to the laser.

The same trend can be observed for the  $\omega>0$  and  $\lambda>0$  cases (e.g. Fig. 2b) but now the spectrum is more complex due to the coupling to light. The lowest states are

$$\begin{split} &\Phi_{c0} \; \approx \; 0.99\phi_0|0\rangle + 0.06\phi_1|1\rangle \\ &\Phi_{c1} \; \approx \; 0.66\phi_1|0\rangle - 0.74\phi_0|1\rangle \\ &\Phi_{c2} \; \approx \; 0.74\phi_1|0\rangle + 0.66\phi_0|1\rangle \\ &\Phi_{c3} \; \approx \; 0.05\phi_0|0\rangle - 0.46\phi_2|0\rangle + 0.71\phi_1|1\rangle \\ &\Phi_{c4} \; \approx \; -0.69\phi_2|0\rangle + 0.08\phi_1|1\rangle + 0.71\phi_0|2\rangle \end{split}$$

(50)

The transition from  $\Phi_{c0}$  to  $\Phi_{c1}$  and  $\Phi_{c2}$  is strong because  $\Phi_{c1}$  and  $\Phi_{c2}$  have large  $\phi_1|0\rangle$  components. These two transition peaks are visible although the first partly overlaps with the peaks at the laser frequency. The excitation energies corresponding to  $\Phi_{c3}$  and  $\Phi_{c4}$  do not appear in the spectrum because the wave function components are much smaller. Transitions from and to other states are also possible but less significant. The excitation energy peaks in Fig. 2c and Fig. 2d can be explained similarly. Compared to Fig. 2b, Fig. 2c is calculated for a smaller cavity frequency. The main effect is that the excitation energies are different and the corresponding peaks are shifted. A similar effect can be observed in Fig. 2d, but in this case the peaks are moved by increasing  $\lambda$ .

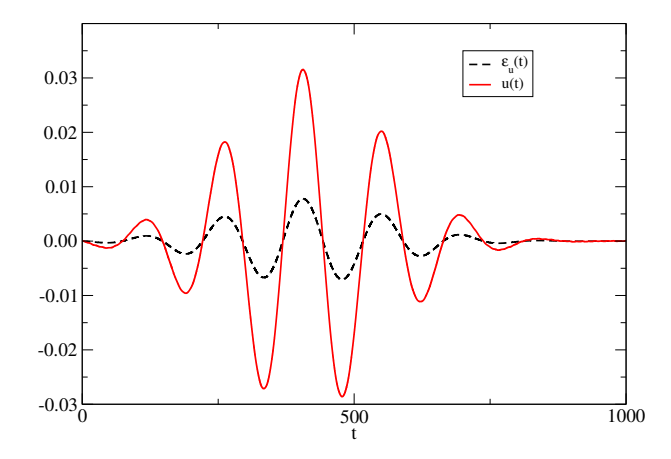


FIG. 3. Polarization and electric field. The laser is defined by Eq. (49) with parameters  $\omega_e = 0.043$ ,  $\tau = 413$  and  $\sigma = 206$ . Laser strength  $E_e = 0.0078$  was used to calculate u(t).

This example shows that the HHG of the system changed in the cavity due to two main effects. The first is that the coupling removed the inversion symmetry restriction, allowing the possible appearance of even harmonics. Secondly, the energy levels of the harmonically confined electrons in the cavity show up in the HHG spectrum. As the energy levels depend on  $\omega_0$ ,  $\omega$ , and  $\lambda$ , one can add HHG peaks at desired positions and can modulate the HHG spectrum with the cavity.

### C. Nonlinear susceptibilities

In this section, we calculate the nonlinear susceptibilities for certain cavity parameters. The nonlinear susceptibilities of molecules in cavities have been studied in Ref. [63]. It was found that the polaritonic resonances can enhance the susceptibilities and the nonlinear conversion efficiency can be tuned by the coupling strength.

Using Eq. (46) we have calculated the polarizations up to the third order. The exciting electric field is typically a few-cycle laser pulse, and the pulse used in this calculation (Eq. (49)) is similar to the choice of Refs. [71, 72]. The frequency of the confining harmonic oscillator potential is chosen to be  $\omega_0 = 0.5$ . The cavity frequency  $\omega$  and the coupling,  $\lambda$ , is selected in such a way that the occupation of the excited state is small. In these cases, the susceptibilities can be extracted using a simple fit. If the excited states are more dominant then the calculation of the frequency-dependent susceptibilities will be more tedious.

Fig. 3 shows the external field and the polarization for a weak laser field. The time-dependent dipole moment smoothly follows the oscillation of the laser. By calculating the dipole moments  $u_i(t)$  for 3 different laser field strengths,  $E_{ei}$  (see Eq. (49)), we can calculate  $p^{(n)}$  using Eq. (45). The values of  $p^{(n)}$  is not sensitive to the values of  $E_{ei}$  provided that the field is sufficiently weak. Fig. 4 shows that  $p^{(n)}$  can be very well approximated by

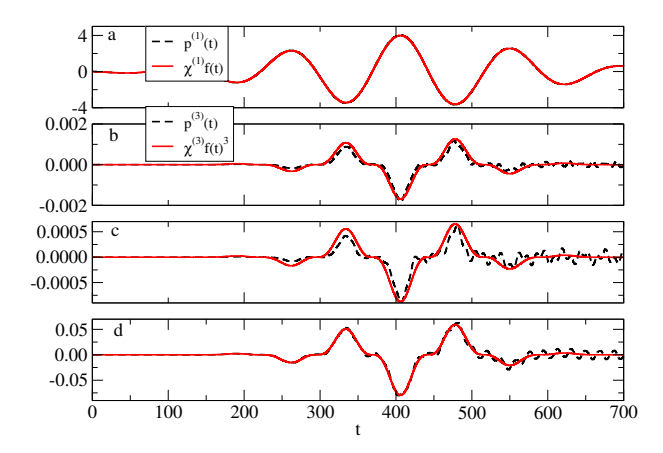


FIG. 4. First and third order susceptibilities. a:  $p^{(1)}(t)$  (dashed black) and  $\chi^{(1)}f(t)$  (red) ( $\chi^{(1)}=4$ ). b:  $p^{(3)}(t)$  (dashed black) and  $\chi^{(3)}f(t)^3$  (red) ( $\chi^{(3)}=0.0017$ ) for  $\omega_0=0.5$ ,  $\omega=0.5$ , and  $\lambda=0.1$ . c:  $p^{(3)}(t)$  (dashed black) and  $\chi^{(3)}f(t)^3$  (red) ( $\chi^{(3)}=0.00088$ ) for  $\omega_0=0.5$ ,  $\omega=0.25$ , and  $\lambda=0.1$ . d:  $p^{(3)}(t)$  (dashed black) and  $\chi^{(3)}f(t)^3$  (red) ( $\chi^{(3)}=0.008$ ) for  $\omega_0=0.5$ ,  $\omega=0.5$ , and  $\lambda=0.2$ . The legend of b is also a legend of c and d. The laser is defined by Eq. (49) with parameters  $\omega_e=0.043$ ,  $\tau=413$  and  $\sigma=206$ . Three laser strengths,  $E_{ei}=0.00195$ , 0.0039, 0.0078 were used to calculate  $p^{(n)}$ .

 $\chi^{(n)}f(t)^n$ , which is a simple time (or frequency) independent susceptibility Fig. 4a shows the linear component,  $\chi^{(1)}=4$  gives an excellent fit to  $p^{(1)}(t)$ . Fig. 4b, 4c and 4d show the dependence of  $p^{(3)}$  on  $\omega$  and  $\lambda$ . These figures show that a simple  $p^{(3)}=\chi^{(3)}f(t)^3$  gives a good fit for the third-order polarization, although the fit is not as perfect as for the first-order one. Note, that while the calculation of the time-dependent dipole is very accurate, the extraction of  $\chi$  one has to be averaged over time which introduces an error bar of about  $\pm 5\%$  due to the fluctuation of the polarization.

Fig. 5 shows the dependence of second and the thirdorder susceptibility on  $\lambda$  and  $\omega$ . The calculations show that the dependence of  $\chi$  on  $\omega$  and  $\lambda$  is closely related to the occupation probability. The value of  $\chi^{(n)}$  increases when the occupation of excited states are higher because more states will be connected with dipole transitions. We have investigated the dependence of the occupation probability on the cavity frequency and coupling in Ref. [55] and now we apply those finding for this case. Fig. 5a shows the occupation of the excited states as a function of  $\omega$ . For a fixed  $\lambda$  two terms in Eq. (30) influence the occupation of the excited states. By increasing  $\omega$ , the second term shifts the energy of the excited states higher and that decreases the occupation probability of the excited states. The third term couples the center-of-mass and the photon spaces and the coupling is proportional to  $\sqrt{\omega}$ . By increasing  $\omega$  the coupling increases and that leads to higher excited state occupation probability. As a result of these two competing processes, the occupation of the excited states first increases with  $\omega$  then reaches a

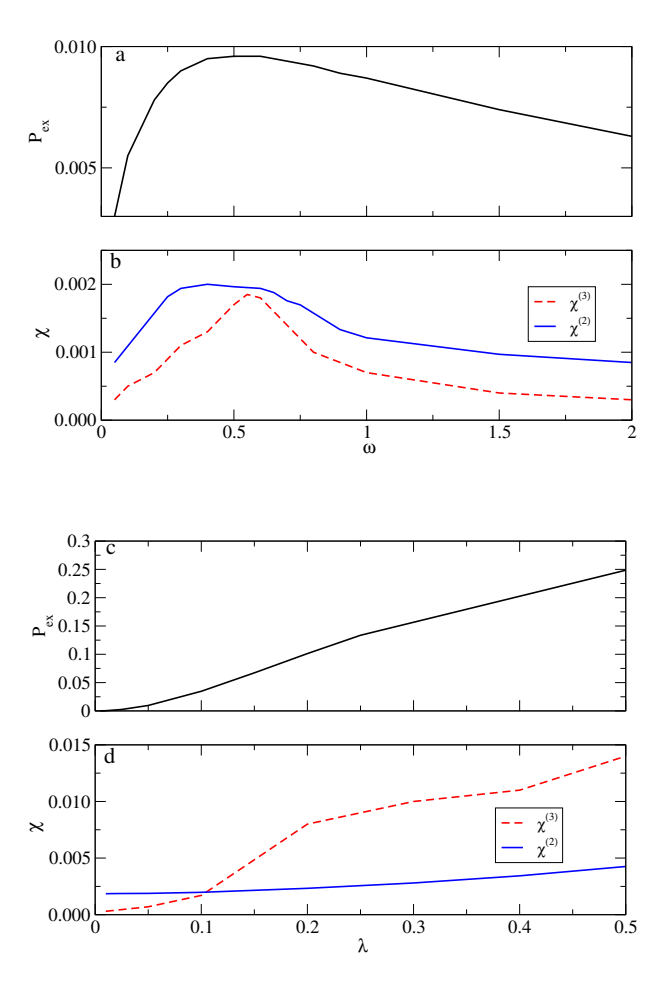


FIG. 5. Dependence of occupation probability of the excited states and the nonlinear susceptibilities  $\chi^{(n)}$  on the cavity frequency and the coupling strength.  $\chi^{(2)}$  is multiplied by 800 to fit in the same figure as  $\chi^{(2)}$ .  $\lambda=0.1$  and  $\omega_0=0.5$  is used for the  $\omega$  dependence and  $\omega=0.5$  and  $\omega_0=0.5$  is used for the  $\lambda$  dependence.

maximum and starts to decrease as it is shown in Fig. 5a. The behavior of  $\chi^{(n)}$  is very similar (Fig. 5b), increasing and reaching a maximum before starting to decrease. The curve is not as smooth as the occupation probability due to the error related to the extraction. A similar behavior can be found for the  $\lambda$  dependence of the occupation number and  $\chi^{(2)}$  (see Figs. 5c and 5d). In this case, the occupation number monotonically increases with  $\lambda$  because the  $\lambda$  is the larger the coupling (third term in Eq. (30)). The second-order polarization,  $\chi^{(2)}$  is much smaller then the third-order one. The small value of the  $chi^{(2)}$  is due to the fact that the second-order process is not allowed without coupling to the cavity and remains hindered for the parameter region of this study.

# V. SUMMARY

We have presented an analytically solvable timedependent model of the interaction of harmonically confined electrons and light in a cavity. In the framework of the Pauli-Fierz Hamiltonian, the relative motion and center-of-mass motion can be factorized. The Hamiltonian of the relative motion is time independent and it is not coupled to light. It can be solved by various approaches as we have described in Refs. [54, 55]. The Hamiltonian of the center-of-mass motion can be written as the sum of three Hamiltonians, each of them depending on a single variable only. This separation allows the factorization of the center-of-mass wave function into a product form so the three Hamiltonians can be solved independently. Two of these Hamiltonians are not coupled to the light and these are simple time-dependent harmonic oscillator Hamiltonians that can be solved analytically (see Appendix C). The third Hamiltonian is a coupled light-matter harmonic oscillator Hamiltonian. This Hamiltonian can be decoupled by using shifted Fock states and it can be solved analytically.

The disadvantage of the analytical solution is that in the wave functions the light and matter coordinates are mixed and it is cumbersome to calculate physical properties in terms of light or matter degrees only. As an alternative, we use a product of harmonic oscillators and Fock states as a basis that allows an exact diagonalization approach. The convergence can be controlled by increasing the number of orthogonal basis states. This product basis can also be used to solve the time-dependent problem with time propagation of the wave function.

Three different time-dependent problems are studied. In the first, we have shown how external fields acting on either the light or the matter degrees of freedom can excite the other degrees of freedom. In the second, the effect of the cavity on the HHG spectrum was investigated. We have shown that with the cavity, one can introduce intensity peaks in the HHG spectrum at desired locations which may have applications in ultrafast (attosecond) spectroscopies. In the third example, we have shown how the third-order nonlinear susceptibility (which is an important quantity controlling nonlinear optical mixing processes) of the system changes and can be tuned in the cavity.

# ACKNOWLEDGMENTS

This work has been supported by the National Science Foundation (NSF) under Grant No. 2217759.

#### Appendix A: Relative coordinates

In a system of N particles with coordinates  $\mathbf{r}_i$  one can introduce N-1 independent relative coordinates  $\mathbf{x}_i$  and a center-of-mass coordinate  $\mathbf{R} = \mathbf{x}_N$  by a linear transformation [73]

$$\mathbf{x}_i = \sum_{j=1}^N U_{ij} \mathbf{r}_j. \tag{A1}$$

Many different choices of definitions of the relative coordinate set are used, for example

$$U = \begin{pmatrix} 1 & -1 & 0 & 0 & \cdots & 0 \\ \frac{1}{2} & \frac{1}{2} & -1 & 0 & \cdots & 0 \\ \vdots & \vdots & \vdots & \ddots & \vdots & 0 \\ \frac{1}{N-1} & \frac{1}{N-1} & \frac{1}{N-1} & \frac{1}{N-1} & \vdots & -1 \\ \frac{1}{N} & \frac{1}{N} & \frac{1}{N} & \frac{1}{N} & \frac{1}{N} & \frac{1}{N} \end{pmatrix},$$

or

$$U' = \begin{pmatrix} 1 - \frac{1}{N} & -\frac{1}{N} & -\frac{1}{N} & \cdots & -\frac{1}{N} \\ -\frac{1}{N} & 1 - \frac{1}{N} & -\frac{1}{N} & \cdots & -\frac{1}{N} \\ \vdots & \vdots & \ddots & \vdots & \vdots \\ -\frac{1}{N} & -\frac{1}{N} & \vdots & 1 - \frac{1}{N} & -\frac{1}{N} \\ \frac{1}{N} & \frac{1}{N} & \frac{1}{N} & \frac{1}{N} & \frac{1}{N} \end{pmatrix},$$

and the generalization for unequal masses is straightforward [73]. The U matrices can be inverted and the different relative coordinates can be transformed into each other. The inverse of the transformation matrices are

$$U^{-1} = \begin{pmatrix} \frac{1}{2} & \frac{1}{3} & \frac{1}{4} & \cdots & \frac{1}{N-1} & 1\\ -\frac{1}{2} & \frac{1}{3} & \frac{1}{4} & \cdots & \frac{1}{N-1} & 1\\ 0 & -\frac{1}{3} & \frac{1}{4} & \cdots & \frac{1}{N-1} & 1\\ \vdots & \vdots & \vdots & \ddots & \vdots & \vdots\\ 0 & 0 & 0 & \cdots & -\frac{N-1}{N} & 1 \end{pmatrix},$$

and

$$U'^{-1} = \begin{pmatrix} 1 & 0 & 0 & \cdots & 0 & 1 \\ 0 & 1 & 0 & \cdots & 0 & 1 \\ 0 & 0 & 1 & \cdots & 0 & 1 \\ \vdots & \vdots & \vdots & \ddots & \vdots & \vdots \\ -1 & -1 & -1 & \cdots & -1 & 1 \end{pmatrix}.$$

As all elements of the last row of U are 1/N, the inverse matrix has a special structure: all elements of its last column is 1 [73]. That means the we can express the single particle coordinates as

$$\mathbf{r}_i = \sum_{j=1}^{N-1} U_{ij}^{-1} \mathbf{x}_j + \mathbf{R}$$
 (A2)

The relative and center-of-mass momenta  $\pi_i = -i\hbar \frac{\partial}{\partial \mathbf{x}_i}$  are related to the single particle momenta  $\mathbf{p}_i = -i\hbar \frac{\partial}{\partial \mathbf{r}_i}$ 

$$\pi_i = \sum_{j=1}^{N} U_{ji}^{-1} \mathbf{p}_j \qquad (i = 1, ...N).$$
(A3)

This equation defines the total momentum as  $\pi_i = \sum_{j=1}^{N} \mathbf{p}_j$  and the center-of-mass kinetic energy is  $T_{cm} = \pi_N^2/2N$ . Now we can subtract the center-of-mass kinetic energy from the total kinetic energy

$$\sum_{i=1}^{N} \frac{\mathbf{p}_i^2}{2} - T_{cm} = \frac{1}{2} \sum_{i=1}^{N-1} \sum_{j=1}^{N-1} \Lambda_{ij} \boldsymbol{\pi}_i \boldsymbol{\pi}_j$$
 (A4)

(B6)

where

$$\Lambda_{ij} = \sum_{k=1}^{N} U_{ik} U_{jk}. \tag{A5}$$

This completes the separation of the relative and centerof-mass system and works in any system defined by U.

As an example let's consider N=3. Using U one can define

$$\mathbf{x}_{1} = \mathbf{r}_{1} - \mathbf{r}_{2},$$

$$\mathbf{x}_{2} = \frac{\mathbf{r}_{1} + \mathbf{r}_{2}}{2} - \mathbf{r}_{3},$$

$$\mathbf{R} = \frac{\mathbf{r}_{1} + \mathbf{r}_{2} + \mathbf{r}_{3}}{3},$$
(A6)

and the single particle coordinates are expressed as

$$\mathbf{r}_{1} = \frac{1}{2}\mathbf{x}_{1} + \frac{1}{3}\mathbf{x}_{2} + \mathbf{R},$$

$$\mathbf{r}_{2} = -\frac{1}{2}\mathbf{x}_{1} + \frac{1}{3}\mathbf{x}_{2} + \mathbf{R},$$

$$\mathbf{r}_{3} = -\frac{2}{3}\mathbf{x}_{2} + \mathbf{R}.$$
(A7)

Similarly, using U' we can define

$$\mathbf{x}'_{1} = \frac{2}{3}\mathbf{r}_{1} - \frac{1}{3}\mathbf{r}_{2} - \frac{1}{3}\mathbf{r}_{3},$$

$$\mathbf{x}'_{2} = -\frac{1}{3}\mathbf{r}_{1} + \frac{2}{3}\mathbf{r}_{2} - \frac{1}{3}\mathbf{r}_{3},$$

$$\mathbf{R} = \frac{\mathbf{r}_{1} + \mathbf{r}_{2} + \mathbf{r}_{3}}{3},$$
(A8)

and now the single particle coordinates are

$$\mathbf{r}_{1} = \mathbf{x}'_{1} + \mathbf{R},$$

$$\mathbf{r}_{2} = \mathbf{x}'_{2} + \mathbf{R},$$

$$\mathbf{r}_{3} = -\mathbf{x}'_{1} - \mathbf{x}'_{2} + \mathbf{R}.$$
(A9)

# Appendix B: Decoupling the center-of-mass Hamiltonian

The center-of-mass part can be simplified further by introducing

$$u = \sqrt{N} \frac{X+Y}{\sqrt{2}}, \quad v = \sqrt{N} \frac{Y-X}{\sqrt{2}}, \quad z = \sqrt{N} Z$$
 (B1)

where  $\mathbf{R} = (X, Y, Z)$ , and

$$\epsilon_{u}(t) = \sqrt{N} \frac{E_{x}(t) + E_{y}(t)}{\sqrt{2}},$$

$$\epsilon_{v}(t) = \sqrt{N} \frac{E_{x}(t) - E_{y}(t)}{\sqrt{2}},$$

$$\epsilon_{z}(t) = \sqrt{N} E_{z}(t),$$
(B3)

where  $\mathbf{E}_{ext}(t) = (E_x(t), E_y(t), E_z(t))$ . Using this notation, the light-matter coupling term becomes

$$\omega q \lambda \mathbf{R} = \omega q \sqrt{2N} \lambda u, \tag{B4}$$

and only the u coordinate is coupled to light. By defining

$$H_{u} = -\frac{1}{2} \frac{\partial^{2}}{\partial u^{2}} + \frac{1}{2} \omega_{u}^{2} u^{2} + \epsilon_{u}(t) u,$$

$$H_{v} = -\frac{1}{2} \frac{\partial^{2}}{\partial v^{2}} + \frac{1}{2} \omega_{v}^{2} v^{2} + \epsilon_{v}(t) v,$$

$$H_{z} = -\frac{1}{2} \frac{\partial^{2}}{\partial z^{2}} + \frac{1}{2} \omega_{z}^{2} z^{2} + \epsilon_{z}(t) z,$$
(B5)

with frequencies

$$\omega_u^2 = \omega_0^2 + 2N\lambda^2, \qquad \omega_v^2 = \omega_z^2 = \omega_0^2,$$
 (B7)

we can write the CM part as

$$H_{\mathbf{R}} + \frac{1}{2}N^2 (\lambda \mathbf{R})^2 = H_u + H_v + H_z.$$
 (B8)

Now the CM Hamiltonian is a sum of three independent time-dependent harmonic oscillators, and only  $H_u$  is coupled with light. This derivation can be easily generalized to any form of  $\lambda$  [54] and is not limited to the present  $\lambda = \lambda(1,1,0)$  choice as we have mentioned before. These time-dependent Hamiltonians have known analytical solutions [67, 68] which have been reviewed in Appendix C. If one choose  $E_x = E_y$  and  $E_z = 0$ , then  $H_v$  and  $H_z$  are time-independent and the solution is even simpler.

Now we can define a simplified coupling Hamiltonian in the following form:

$$H_c = \omega \left( \hat{a}^+ \hat{a} + \frac{1}{2} \right) - \omega q \sqrt{2N} \lambda u + \frac{j_{\text{ext}}(t)}{\omega} \hat{q} + H_u.$$
 (B9)

The total Hamiltonian now becomes

$$H = H_{\mathbf{x}} + H_v + H_z + H_c, \tag{B10}$$

By solving the Schrödinger equation for the time-independent part

$$H_{\mathbf{x}}\Phi(\mathbf{x}) = E_{\mathbf{x}}\Phi(\mathbf{x}) \tag{B11}$$

and solving the time-dependent Schrödinger equations for the time dependent parts

$$i\frac{\partial}{\partial t}\phi_v(v,t) = H_v\phi_v(v,t)$$
 (B12)

$$i\frac{\partial}{\partial t}\phi_z(z,t) = H_z\phi_z(z,t)$$
 (B13)

$$i\frac{\partial}{\partial t}\Phi_c(u,t) = H_c\Phi_c(u,t).$$
 (B14)

The ansatz

$$\Psi = \Phi(\mathbf{x})e^{-iE_{\mathbf{x}}t}\phi_v(v,t)\phi_z(z,t)\Phi_c(u,t),$$
 (B15)

satisfies the time-dependent Schrödinger equation

$$i\frac{\partial}{\partial t}\Psi = H\Psi. \tag{B16}$$

# Appendix C: Solution of the time-dependent harmonic oscillator Hamiltonian

The time-dependent Schrödinger equation for a harmonic oscillator driven by a laser field is analytically solvable [67, 68]. We include the key ingredients in this Appendix for completeness. The starting equation is

$$-\frac{\hbar^2}{2m}\frac{\partial^2}{\partial x^2} + \left[\frac{1}{2}kx^2 - xF(t)\right]\psi = i\hbar\frac{\partial\psi}{\partial t},\tag{C1}$$

where F(t) is a time-dependent driving field. Rewrite  $\psi$  into the form

$$\psi(x,t) = \chi(x,t)e^{g(t)x}$$
  $\chi(x,t) = \phi(x - u(t), t), (C2)$ 

where u(t) and g(t) are auxiliary functions to be determined. By substituting this ansatz into Eq. (C1), one has

$$-\frac{\hbar^2}{2m}\frac{\partial^2\phi}{\partial\xi^2} + \left(i\hbar\dot{u} - \frac{\hbar^2}{m}g\right)\frac{\partial\phi}{\partial\xi} + \frac{1}{2}k\xi^2\phi$$

$$+ (ku - F - i\hbar\dot{g})\xi\phi$$

$$+ \left(\frac{1}{2}ku^2 - Fu - i\hbar u\dot{g} - \frac{\hbar^2}{2m}g^2\right)\phi = i\hbar\frac{\partial\phi}{\partial t}, (C3)$$

where  $\xi = x - u(t)$ . Now we can choose g and u to eliminate the coefficients of  $\partial \phi / \partial \xi$  and  $\xi \phi$ ,

$$i\hbar\dot{u} - \frac{\hbar^2}{m}g = 0, \quad ku - F - i\hbar\dot{g} = 0$$
 (C4)

and Eq. (C3) simplifies to

$$-\frac{\hbar^2}{2m}\frac{\partial^2\phi}{\partial\xi^2} + \frac{1}{2}k\xi^2\phi = i\hbar\frac{\partial\phi}{\partial t} - \delta(t)\phi, \tag{C5}$$

where we have defined

$$\delta(t) = \frac{1}{2}ku^2 - Fu - i\hbar u\dot{g} - \frac{\hbar^2}{2m}g^2 = \frac{1}{2}m\dot{u}^2 - \frac{1}{2}ku^2 \text{ (C6)}$$

where the second equality is obtained by using Eqs. (C4).

In Eq. (C5), the  $\xi$  and t variables are separable, and the left-hand side represents the time-independent harmonic oscillators, with eigenenergies  $E_n = \left(n + \frac{1}{2}\right)\hbar\omega$  and wave functions

$$N_n \exp\left(-\frac{1}{2}\alpha^2\xi^2\right) H_n(\alpha\xi)$$
 (C7)

where  $H_n$  is the *n*th Hermite polynomial,

$$\alpha^4 = mk/\hbar^2, \qquad \omega = [k/m]^{\frac{1}{2}},$$
 (C8)

$$N_{n^2} = \frac{\alpha}{\pi^{\frac{1}{2}} 2^n n!}.$$
 (C9)

The right-hand side can be integrated over time, and the total solution is

$$\phi = N_n \exp\left\{-\frac{i}{\hbar} \int \left[\delta(t) + E_n\right] dt\right\} \exp\left(-\frac{1}{2}\alpha^2 \xi^2\right) H_n(\alpha \xi)$$
(C10)

Note that Eq. (C4) is equivalent to a driven classical harmonic oscillator equation

$$m\ddot{u} + ku = F(t), \tag{C11}$$

and g is also uniquely determined by solving for u in this equation.

As a simple example, we consider a sinusoidal driving field of the electrons:  $\epsilon_q = 0$ ,  $\epsilon_u = C_F \cos(\omega_F t)$  in (19). The transformed driving fields  $c_r(t)$ ,  $c_s(t)$ , corresponding to F(t) above, are still of the form  $C_F \cos(\omega_F t)$ . The solution to (C11) is well-known:

$$u = A_1 \exp(i\omega t) + A_2 \exp(-i\omega t) + \frac{C_F}{|\omega^2 - \omega_F^2|} \cos(\omega_F t),$$
(C12)

where  $A_1$ ,  $A_2$  are given by the initial conditions, and  $\omega$  is the oscillator frequency. Note that the complex parts of u should not be dropped, as they affect the time-dependency of the wave functions. One can easily evaluate the integral:

$$\int \delta(t)dt = \frac{i\omega}{2} (A_1^2 e^{2i\omega t} - A_2^2 e^{-2i\omega t})$$

$$- \frac{C_F^2 t}{4(\omega^2 - \omega_F^2)} - \frac{C_F^2 (\omega^2 + \omega_F^2)}{8\omega_F (\omega^2 - \omega_F^2)^2} \sin(2\omega_F t)$$

$$+ \frac{i\omega C_F (A_1 e^{i\omega t} - A_2 e^{-i\omega t})}{|\omega^2 - \omega_F^2|} \cos(\omega_F t)$$
(C13)

Thus, the time-dependent wave function is determined.

In our case, the analytical solution for  $H_c$  (Eq. (23)) can be written as a product of the eigen functions of  $H_r$  and  $H_s$ 

$$\Phi_c = \chi_r \chi_s \phi_{r,n} \phi_{s,m}, \tag{C14}$$

where

$$\phi_{r,n} = N_{r,n} \exp\left\{-i \int \left[\delta_r(t) + E_n\right] dt - \frac{1}{2}\omega_r \xi_r^2\right\} H_n(\sqrt{\omega_r}\xi_r),$$
(C15)

$$N_{r,n} = \left(\frac{\omega_r}{\pi}\right)^{\frac{1}{4}} \frac{1}{\sqrt{2^n n!}}, \ E_n = \left(n + \frac{1}{2}\right) \omega_r,$$

$$\delta_r(t) = \frac{1}{2} \dot{w}^2 - \frac{1}{2} \omega_r^2 w^2, \ \xi_r(t) = r - w(t),$$
(C16)

$$\chi_r = \exp(ir\dot{w}). \tag{C17}$$

 $H_n$  is the n-th Hermite polynomials, and w(t) is the solution to  $\ddot{w} + \omega_r^2 w = -c_r(t)$ , which has exact particular solutions in integral form for any reasonable  $c_r(t)$ . Appendix C shows an analytical example. The  $\chi_s$  and  $\phi_{s,m}$  are obtained analogously. In principle, any starting wave function can be decomposed through a basis formed by  $\phi_{r,n}$  at t=0 and time propagated by evolving each  $\phi_{r,n}$ .

# Appendix D: Decoupling

Suppose the following Hamiltonian

$$H = -\frac{1}{2}\frac{\partial^2}{\partial x^2} - \frac{1}{2}\frac{\partial^2}{\partial y^2} + \frac{1}{2}\omega_x^2 x^2 + \frac{1}{2}\omega_y^2 y^2 + kxy + a(t)x + b(t)y$$
(D1)

Assume the following transformations:

$$u = x \cos \theta - y \sin \theta$$
  

$$v = x \sin \theta + y \cos \theta$$
 (D2)

Then we decouple the Hamiltonian

$$H = H_u + H_v \tag{D3}$$

where

$$\begin{split} H_{u} &= -\frac{1}{2} \frac{\partial^{2}}{\partial u^{2}} + \frac{1}{2} \omega_{u}^{2} u^{2} + c(t) u \\ H_{v} &= -\frac{1}{2} \frac{\partial^{2}}{\partial v^{2}} + \frac{1}{2} \omega_{v}^{2} v^{2} + d(t) v \end{split} \tag{D4}$$

and

$$c = a\cos\theta - b\sin\theta, \ d = a\sin\theta + b\cos\theta$$
 (D5)

The rotational angle is given by

$$\tan 2\theta = -\frac{2k}{\omega_x^2 - \omega_y^2} \tag{D6}$$

and the frequencies

$$\omega_u^2 = \omega_x^2 \cos^2 \theta + \omega_y^2 \sin^2 \theta - k \sin 2\theta$$
 (D7)

$$\omega_v^2 = \omega_x^2 \sin^2 \theta + \omega_y^2 \cos^2 \theta + k \sin 2\theta$$
 (D8)

 $H_u$  and  $H_v$  can be solved by Appendix C

- [1] E. Jaynes and F. Cummings, Comparison of quantum and semiclassical radiation theories with application to the beam maser, Proceedings of the IEEE **51**, 89 (1963).
- [2] S. Haroche and J. Raimond, Radiative properties of rydberg states in resonant cavities (Academic Press, 1985) pp. 347–411.
- [3] D. Meschede, H. Walther, and G. Müller, One-atom maser, Phys. Rev. Lett. 54, 551 (1985).
- [4] G. Rempe, H. Walther, and N. Klein, Observation of quantum collapse and revival in a one-atom maser, Phys. Rev. Lett. 58, 353 (1987).
- [5] I. I. Rabi, On the process of space quantization, Phys. Rev. 49, 324 (1936).
- [6] J. J. Slosser, P. Meystre, and S. L. Braunstein, Harmonic oscillator driven by a quantum current, Phys. Rev. Lett. 63, 934 (1989).
- [7] S. Brattke, B. T. H. Varcoe, and H. Walther, Generation of photon number states on demand via cavity quantum electrodynamics, Phys. Rev. Lett. 86, 3534 (2001).
- [8] M. Weidinger, B. T. H. Varcoe, R. Heerlein, and H. Walther, Trapping states in the micromaser, Phys. Rev. Lett. 82, 3795 (1999).
- [9] M. Hillery, Squeezing and photon number in the jaynescummings model, Phys. Rev. A 39, 1556 (1989).
- [10] S. Bose, I. Fuentes-Guridi, P. L. Knight, and V. Vedral, Subsystem purity as an enforcer of entanglement, Phys. Rev. Lett. 87, 050401 (2001).
- [11] M. Brune, S. Haroche, J. M. Raimond, L. Davidovich, and N. Zagury, Manipulation of photons in a cavity by dispersive atom-field coupling: Quantum-nondemolition measurements and generation of "schrödinger cat" states, Phys. Rev. A 45, 5193 (1992).
- [12] F. m. c. Dubin, D. Rotter, M. Mukherjee, C. Russo, J. Eschner, and R. Blatt, Photon correlation versus interference of single-atom fluorescence in a half-cavity, Phys. Rev. Lett. 98, 183003 (2007).
- [13] M. Hennrich, A. Kuhn, and G. Rempe, Transition from antibunching to bunching in cavity qed, Phys. Rev. Lett.

- **94**, 053604 (2005).
- [14] F. Krumm and W. Vogel, Time-dependent nonlinear jaynes-cummings dynamics of a trapped ion, Phys. Rev. A 97, 043806 (2018).
- [15] A. Joshi, Nonlinear dynamical evolution of the driven two-photon jaynes-cummings model, Phys. Rev. A 62, 043812 (2000).
- [16] M. S. Abdalla, E. Khalil, and A.-F. Obada, Exact treatment of the jaynes-cummings model under the action of an external classical field, Annals of Physics 326, 2486 (2011).
- [17] F.-l. Li and S.-y. Gao, Controlling nonclassical properties of the jaynes-cummings model by an external coherent field, Phys. Rev. A 62, 043809 (2000).
- [18] C. A. Blockley, D. F. Walls, and H. Risken, Quantum collapses and revivals in a quantized trap, Europhysics Letters 17, 509 (1992).
- [19] L. Ermann, G. G. Carlo, A. D. Chepelianskii, and D. L. Shepelyansky, Jaynes-cummings model under monochromatic driving, Phys. Rev. A 102, 033729 (2020).
- [20] O. V. Zhirov and D. L. Shepelyansky, Synchronization and bistability of a qubit coupled to a driven dissipative oscillator, Phys. Rev. Lett. 100, 014101 (2008).
- [21] A. Joshi and S. V. Lawande, Generalized jaynescummings models with a time-dependent atom-field coupling, Phys. Rev. A 48, 2276 (1993).
- [22] Y. Yang, J. Xu, G. Li, and H. Chen, Interactions of a two-level atom and a field with a time-varying frequency, Phys. Rev. A 69, 053406 (2004).
- [23] P. Alsing, D.-S. Guo, and H. J. Carmichael, Dynamic stark effect for the jaynes-cummings system, Phys. Rev. A 45, 5135 (1992).
- [24] D. Pagel, A. Alvermann, and H. Fehske, Dynamic stark effect, light emission, and entanglement generation in a laser-driven quantum optical system, Phys. Rev. A 95, 013825 (2017).
- [25] T. K. Mavrogordatos, Strong-coupling limit of the driven dissipative light-matter interaction, Phys. Rev. A 100,

- 033810 (2019).
- [26] H. R. Baghshahi, M. K. Tavassoly, and S. J. Akhtarshenas, Generation and nonclassicality of entangled states via the interaction of two three-level atoms with a quantized cavity field assisted by a driving external classical field, Quantum Information Processing 14, 1279 (2015).
- [27] A. T. Avelar and B. Baseia, Preparing highly excited fock states of a cavity field using driven atoms, Journal of Optics B: Quantum and Semiclassical Optics 7, 198
- [28] C. C. Gerry, Conditional state generation in a dispersive atom-cavity field interaction with a continuous external pump field, Phys. Rev. A 65, 063801 (2002).
- [29] H. Nha, Y.-T. Chough, W. Jhe, and K. An, Dynamically induced atomic resonance fluorescence and cavity transmission spectra in a driven jaynes-cummings system, Phys. Rev. A 63, 063814 (2001).
- [30] C. K. Law and J. H. Eberly, Arbitrary control of a quantum electromagnetic field, Phys. Rev. Lett. 76, 1055 (1996).
- [31] J. A. Hutchison, T. Schwartz, C. Genet, E. Devaux, and T. W. Ebbesen, Modifying chemical landscapes by coupling to vacuum fields, Angewandte Chemie International Edition **51**, 1592 (2012).
- [32] R. Balili, V. Hartwell, D. Snoke, L. Pfeiffer, and K. West, Bose-einstein condensation of microcavity polaritons in a trap, Science 316, 1007 (2007), https://science.sciencemag.org/content/316/5827/1007.full.pdf.
- [33] J. Schachenmayer, C. Genes, E. Tignone, and G. Pupillo, Cavity-enhanced transport of excitons, Phys. Rev. Lett. **114**, 196403 (2015).
- [34] B. Xiang, R. F. Ribeiro, M. Du, L. Chen, Z. Yang, J. Wang, J. Yuen-Zhou, and W. Xiong, Intermolecular vibrational energy transfer enabled by microcavity strong light-matter coupling, Science 368, 665 (2020), https://science.sciencemag.org/content/368/6491/665.full.pdf.
- [35] A. Reserbat-Plantey, I. Epstein, I. Torre, A. T. Costa, P. A. D. Gonçalves, N. A. Mortensen, M. Polini, J. C. W. Song, N. M. R. Peres, and F. H. L. Koppens, Quantum nanophotonics in two-dimensional materials, ACS Photonics 8, 85 (2021).
- [36] D. M. Coles, N. Somaschi, P. Michetti, C. Clark, P. G. Lagoudakis, P. G. Savvidis, and D. G. Lidzey, Polaritonmediated energy transfer between organic dyes in a strongly coupled optical microcavity, Nature Materials **13**, 712 (2014).
- [37] J. Kasprzak, M. Richard, S. Kundermann, A. Baas, P. Jeambrun, J. M. J. Keeling, F. M. Marchetti, M. H. Szymańska, R. André, J. L. Staehli, V. Savona, P. B. Littlewood, B. Deveaud, and L. S. Dang, Bose-einstein condensation of exciton polaritons, Nature 443, 409 (2006).
- [38] T. Schwartz, J. A. Hutchison, C. Genet, and T. W. Ebbesen, Reversible switching of ultrastrong light-molecule coupling, Phys. Rev. Lett. 106, 196405 (2011).
- [39] J. D. Plumhof, T. Stöferle, L. Mai, U. Scherf, and R. F. Mahrt, Room-temperature bose-einstein condensation of cavity exciton-polaritons in a polymer, Nature Materials **13**, 247 (2014).
- [40] J. A. Hutchison, A. Liscio, T. Schwartz, A. Canaguier-Durand, C. Genet, V. Palermo, P. Samorì, and T. W. Ebbesen, Tuning the work-function strong coupling, Advanced Materials 25, 2481 (2013), https://onlinelibrary.wiley.com/doi/pdf/10.1002/adma.201203682effective potentials in real space, Proceedings of the

- [41] K. Wang, M. Seidel, K. Nagarajan, T. Chervy, C. Genet, and T. Ebbesen, Large optical nonlinearity enhancement under electronic strong coupling, Nature Communications 12, 1486 (2021).
- [42] D. N. Basov, A. Asenjo-Garcia, P. J. Schuck, X. Zhu, and A. Rubio, Polariton panorama, Nanophotonics 10, 549 (2021).
- [43] D. Craig and T. Thirunamachandran, Molecular Quantum Electrodynamics; An Introduction to Radiation Molecule Interactions (1984).
- [44] M. Ruggenthaler, N. Tancogne-Dejean, J. Flick, H. Appel, and A. Rubio, From a quantum-electrodynamical light-matter description to novel spectroscopies, Nature Reviews Chemistry 2, 0118 (2018).
- [45] V. Rokaj, D. M. Welakuh, M. Ruggenthaler, and A. Rubio, Light-matter interaction in the long-wavelength limit: no ground-state without dipole self-energy, Journal of Physics B: Atomic, Molecular and Optical Physics **51**, 034005 (2018).
- [46] A. Mandal, S. Montillo Vega, and P. Huo, Polarized fock states and the dynamical casimir effect in molecular cavity quantum electrodynamics, The Journal of Physical Chemistry Letters 11, 9215 (2020), pMID: 32991814.
- [47] A. Mandal, T. D. Krauss, and P. Huo, Polaritonmediated electron transfer via cavity quantum electrodynamics, The Journal of Physical Chemistry B 124, 6321 (2020), pMID: 32589846.
- [48] I. V. Tokatly, Conserving approximations in cavity quantum electrodynamics: Implications for density functional theory of electron-photon systems, Phys. Rev. B 98, 235123 (2018).
- [49] D. S. Wang, T. Neuman, J. Flick, and P. Narang, Light-matter interaction of a molecule in a dissipative cavity from first principles. The Journal of Chemical Physics **154**, 104109 (2021).
- [50] J. Flick and P. Narang, Ab initio polaritonic potentialenergy surfaces for excited-state nanophotonics and polaritonic chemistry, The Journal of Chemical Physics **153**, 094116 (2020).
- [51] N. Rivera, J. Flick, and P. Narang, Variational theory of nonrelativistic quantum electrodynamics, Phys. Rev. Lett. 122, 193603 (2019).
- [52] J. Flick, N. Rivera, and P. Narang, Strong light-matter coupling in quantum chemistry and quantum photonics, Nanophotonics 7, 1479 (2018).
- [53] J. Flick and P. Narang, Cavity-correlated electronnuclear dynamics from first principles, Phys. Rev. Lett. **121**, 113002 (2018).
- [54] C. Huang, A. Ahrens, M. Beutel, and K. Varga, Two electrons in harmonic confinement coupled to light in a cavity, Phys. Rev. B 104, 165147 (2021).
- [55] J. Malave, Y. S. Aklilu, M. Beutel, C. Huang, and K. Varga, Harmonically confined n-electron systems coupled to light in a cavity, Phys. Rev. B 105, 115127 (2022).
- [56] H. Gao, F. Schlawin, M. Buzzi, A. Cavalleri, and D. Jaksch, Photoinduced electron pairing in a driven cavity, Phys. Rev. Lett. 125, 053602 (2020).
- [57] V. Rokaj, M. Ruggenthaler, F. G. Eich, and A. Rubio, Free electron gas in cavity quantum electrodynamics, Phys. Rev. Research 4, 013012 (2022).
- [58] J. Flick, M. Ruggenthaler, H. Appel, and A. Rubio, Kohn-sham approach to quantum electrodynamical density-functional theory: Exact time-dependent

- National Academy of Sciences 112, 15285 (2015), https://www.pnas.org/content/112/50/15285.full.pdf.
- [59] J. Keller, G. Scalari, S. Cibella, C. Maissen, F. Appugliese, E. Giovine, R. Leoni, M. Beck, and J. Faist, Few-electron ultrastrong light-matter coupling at 300 ghz with nanogap hybrid lc microcavities, Nano Letters 17, 7410 (2017), pMID: 29172537.
- [60] M. Halbhuber, J. Mornhinweg, V. Zeller, C. Ciuti, D. Bougeard, R. Huber, and C. Lange, Non-adiabatic stripping of a cavity field from electrons in the deepstrong coupling regime, Nature Photonics 14, 675 (2020).
- [61] J. Mornhinweg, M. Halbhuber, C. Ciuti, D. Bougeard, R. Huber, and C. Lange, Tailored subcycle nonlinearities of ultrastrong light-matter coupling, Phys. Rev. Lett. 126, 177404 (2021).
- [62] J. Keller, G. Scalari, S. Cibella, F. Appugliese, C. Maissen, E. Giovine, R. Leoni, M. Beck, and J. Faist, Hybrid nano-gap lc-metasurface at 300 ghz ultrastrongly coupled to less than 100 electrons, in Advanced Photonics 2018 (BGPP, IPR, NP, NOMA, Sensors, Networks, SPPCom, SOF) (Optica Publishing Group, 2018) p. NoM4J.3.
- [63] D. M. Welakuh and P. Narang, Tunable nonlinearity and efficient harmonic generation from a strongly coupled light-matter system, ACS Photonics 10, 383 (2023).
- [64] J. Flick, Ruggenthaler, H. Μ. Appel, A. Rubio, Atoms and molecules in cavities, strong coupling in quantumfrom weak to chemistry, Proceedings of electrodynamics (qed)the National Academy of Sciences 114, 3026 (2017), https://www.pnas.org/content/114/12/3026.full.pdf.

- [65] C. Schafer, M. Ruggenthaler, and A. Rubio, Ab initio nonrelativistic quantum electrodynamics: Bridging quantum chemistry and quantum optics from weak to strong coupling, Phys. Rev. A 98, 043801 (2018).
- [66] M. Ruggenthaler, J. Flick, C. Pellegrini, H. Appel, I. V. Tokatly, and A. Rubio, Quantum-electrodynamical density-functional theory: Bridging quantum optics and electronic-structure theory, Phys. Rev. A 90, 012508 (2014).
- [67] K. Husimi, Miscellanea in Elementary Quantum Mechanics, II, Progress of Theoretical Physics 9, 381 (1953), https://academic.oup.com/ptp/articlepdf/9/4/381/5231296/9-4-381.pdf.
- [68] E. H. Kerner, Note on the forced and damped oscillator in quantum mechanics, Canadian Journal of Physics 36, 371 (1958).
- [69] J. Crank and P. Nicolson, A practical method for numerical evaluation of solutions of partial differential equations of the heat-conduction type, Mathematical Proceedings of the Cambridge Philosophical Society 43, 50–67 (1947).
- [70] D. Kidd, C. Covington, and K. Varga, Exponential integrators in time-dependent density-functional calculations, Phys. Rev. E 96, 063307 (2017).
- [71] M. Uemoto, Y. Kuwabara, S. A. Sato, and K. Yabana, Nonlinear polarization evolution using time-dependent density functional theory, The Journal of Chemical Physics 150, 094101 (2019).
- [72] V. A. Goncharov and K. Varga, Real-space, real-time calculation of dynamic hyperpolarizabilities, The Journal of Chemical Physics 137, 094111 (2012).
- [73] Y. Suzuki, M. Suzuki, and K. Varga, Stochastic variational approach to quantum-mechanical few-body problems, Vol. 54 (Springer Science & Business Media, 1998).